the plant journal

SEB Society for Experimental Biology

The Plant Journal (2014) **78,** 850–864 doi: 10.1111/tpj.12510

Identification and suppression of the *p*-coumaroyl CoA: hydroxycinnamyl alcohol transferase in *Zea mays* L.

Jane M. Marita[1,*], Ronald D. Hatfield[1], David M. Rancour[1] and Kenneth E. Frost[2]

[1]*US Department of Agriculture/Agricultural Research Service, US Dairy Forage Research Center, 1925 Linden Drive, Madison, WI 53706, USA, and*

[2]*Plant Pathology, University of Wisconsin Madison, Madison, WI 53706, USA*

Received 26 November 2013; revised 7 March 2014; accepted 12 March 2014; published online 22 March 2014.

*For correspondence (e-mail j.marita@ars.usda.gov).

SUMMARY

Grasses, such as *Zea mays* L. (maize), contain relatively high levels of *p*-coumarates (*p*CA) within their cell walls. Incorporation of *p*CA into cell walls is believed to be due to a hydroxycinnamyl transferase that couples *p*CA to monolignols. To understand the role of *p*CA in maize development, the *p*-coumaroyl CoA: hydroxycinnamyl alcohol transferase (*p*CAT) was isolated and purified from maize stems. Purified *p*CAT was subjected to partial trypsin digestion, and peptides were sequenced by tandem mass spectrometry. TBLASTN analysis of the acquired peptide sequences identified a single full-length maize cDNA clone encoding all the peptide sequences obtained from the purified enzyme. The cDNA clone was obtained and used to generate an RNAi construct for suppressing *p*CAT expression in maize. Here we describe the effects of suppression of *p*CAT in maize. Primary screening of transgenic maize seedling leaves using a new rapid analytical platform was used to identify plants with decreased amounts of *p*CA. Using this screening method, mature leaves from fully developed plants were analyzed, confirming reduced *p*CA levels throughout plant development. Complete analysis of isolated cell walls from mature transgenic stems and leaves revealed that lignin levels did not change, but *p*CA levels decreased and the lignin composition was altered. Transgenic plants with the lowest levels of *p*CA had decreased levels of syringyl units in the lignin. Thus, altering the levels of *p*CAT expression in maize leads to altered lignin composition, but does not appear to alter the total amount of lignin present in the cell walls.

Keywords: *p*-coumarate, transferase, cell wall, lignin, *p*-coumaroylation, *Zea mays* L., accession number BT042717.1.

INTRODUCTION

Hydroxycinnamates are a common component of plant cell walls among members of the Poaceae (grass) family (Harris and Hartley, 1980; Hatfield *et al.*, 2009). The two most prominent compounds are *p*-coumaric acid (4-hydroxycinnamic acid, *p*CA) and ferulic acid (3-methoxy-4-hydroxycinnamic acid, FA). Initially it was assumed that both acids were esterified to carbohydrates within the cell wall, forming hydroxycinnamates (Mueller-Harvey *et al.*, 1986). However, subsequently, it was shown *p*CA is almost exclusively esterified to lignin, and only ferulic acid is esterified to carbohydrates in the cell wall (Lu and Ralph, 1999). The *p*CA remains attached only through its ester linkage, and is uncoupled from other cell-wall components including itself (Lu and Ralph, 1999). There have been reports of cyclodimer formation between *p*CA and FA, but these are usually minor forms of cross-linking within the cell wall (Ford and Hartley, 1989, 1990; Hatfield *et al.*, 1999b).

*p*CA is incorporated into the cell wall as a conjugate with monolignols, especially sinapyl alcohol (SA) (Ralph *et al.*, 1994; Hatfield *et al.*, 2009). During the process of radical-mediated coupling of lignin, the monolignol portion is incorporated into the expanding lignin molecule but the *p*CA end remains unattached (Hatfield *et al.*, 2008a). Recent work indicated that *p*CA may aid in formation of syringyl (S)-type lignin in maize (Hatfield *et al.*, 2008a). Cell-wall peroxidases do not oxidize SA as readily as coniferyl alcohol (CA), FA and *p*CA (50-fold less). Earlier work also demonstrated enhanced oxidation of SA when hydroxycinnamates (e.g. *p*CA and FA) were added to a reaction mixture of hydrogen peroxide, peroxidase and sinapyl alcohol (Takahama *et al.*, 1996; Takahama and Oniki, 1997). Due to differences in redox potentials, *p*CA may readily transfer its radical state to SA. Therefore the *p*-coumarate-sinapyl alcohol (*p*CA-SA) conjugate may act as a radical shuttle,

passing its radical state after oxidation of the *p*CA residue onto SA moieties multiple times.

A crop such as maize (a C4 plant) has high levels of *p*CA compared to plants such as *Dactylis glomerata* L. (orchard grass, a C3 plant), which has 40–50% lower levels. Evaluation of multiple C3 and C4 grasses (Hatfield *et al.*, 2009) indicated no correlation between whether a grass was C3 or C4 and its levels of *p*CA. The highest level of *p*CA incorporation in C3 grasses is significantly less than the highest level in the C4 group, as a percentage difference (Hatfield *et al.*, 2009).

With *p*CA present almost exclusively on lignin in grasses, a correlation between the amount of lignin and *p*CA in the cell wall may be expected. Although this holds reasonably well within a species (Jung and Casler, 1991; Marita *et al.*, 2003), this relationship does not hold across species. A comparison of maize stems with orchard grass stems shows a sixfold higher level of *p*CA in maize but only a 10–20% higher level of lignin (Hatfield *et al.*, 2009). Because a large proportion of *p*CA forms conjugates with SA preferentially over CA, correlations between *p*CA and S units in lignin may be more meaningful. However, the method of analysis used to determine the amount of SA and CA in lignin (i.e. thioacidolysis or nitrobenzene oxidation) may skew the results, as no individual wet chemical method releases all of the SA and CA that make up lignin (Obst, 1982; Lin and Dence, 1992).

Maize silage is used as a forage source in most dairy rations in the USA, and this work was undertaken to increase our knowledge of cell walls in maize, particularly the role of *p*CA in grass cell walls. A study by Withers *et al.* (2012) identified an *Oryza sativa* L. (rice) gene for an enzyme that acylates monolignols with *p*-coumarates. Although the gene was expressed in *Escherichia coli* and the enzyme was characterized, no *in planta* work was performed to determine its activity levels. Due to its economic importance and role as a model for C4 grasses, maize was used as our plant model to test hypotheses concerning the formation of *p*CA-SA conjugates, the gene involved, and incorporation into the cell wall. Here we describe the isolation and characterization of a *p*-coumaroyl CoA:hydroxycinnamyl alcohol transferase (*p*CAT) responsible for formation of *p*CA-monolignol conjugates in maize. We describe purification of the transferase protein, proteomic peptide characterization, and gene identification. We also describe RNAi-mediated suppression of the *p*CAT gene in maize, and the effects of suppression on *p*CA and lignin levels in isolated maize cell walls.

RESULTS AND DISCUSSION

Previous work showed that incorporation of *p*CA into grass cell walls is dependent on formation of *p*CA monolignol conjugates (primarily *p*CA-SA) and subsequent incorporation in the growing lignin polymer during cell-wall development (Lu and Ralph, 1999; Hatfield *et al.*, 2008a). Only the monolignol portion of the conjugate is incorporated into lignin, leaving the *p*CA simply attached by an ester linkage. Therefore, incorporation of *p*CA into cell walls is dependent upon a putative *p*CAT enzyme. When selecting maize for this work, the consistency of *p*CAT activity in the stem material outweighed any difficulty in purifying the enzyme due to apparent low levels of *p*CAT protein and enzyme activity in the stem (Hatfield *et al.*, 2008b).

Purification, enzyme activity, and protein identification of the maize transferase

Several steps were used to isolate the *p*CAT activity from all other proteins: (1) crude protein extraction, (2) ammonium sulfate precipitation, (3) DEAE 650M ion-exchange chromatography, (4) butyl Sepharose hydrophobic interaction, (5) Sephacryl size-exclusion chromatography, (6) Reactive affinity Yellow dye # 3 chromatography, and (7) Uno Q1R ion-exchange chromatography. This purification scheme resulted in a >1000-fold increase in specific activity. Analysis of purified protein fractions by SDS-PAGE (Figure 1) revealed a single protein band of size similar to the estimated molecular weight obtained by size-exclusion chromatography of eluted activity and published *p*CAT enzymes at that time (Yang and Fujita, 1997; Back *et al.*, 2001; D'Auria *et al.*, 2007).

To determine the specificity of *p*CAT, acceptor molecules and CoA donor molecules were tested (Figure 2). Estimations of product formation were based upon HPLC analysis to monitor acceptor molecule disappearance and conjugate formation. Previous work with hydroxycinnamoyl CoA donor molecules indicated that SA or CA conjugates do not survive derivatization/GLC analysis, preventing characterization of products by GC-MS (Hatfield *et al.*, 2009). However, it was shown that dihydrohydroxycinnamyl alcohols

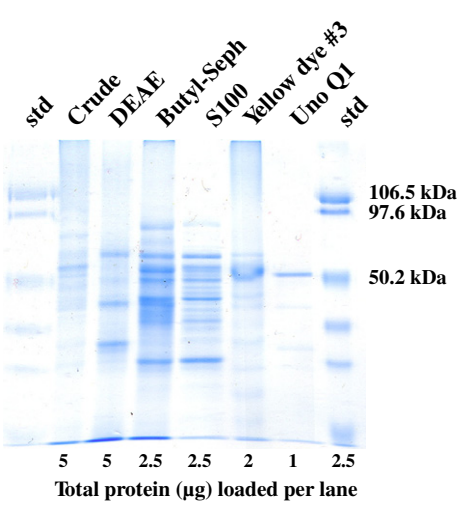

Figure 1. SDS-PAGE for the various steps involved in obtaining purified *p*-coumaroyl CoA:hydroxycinnamyl alcohol transferase.

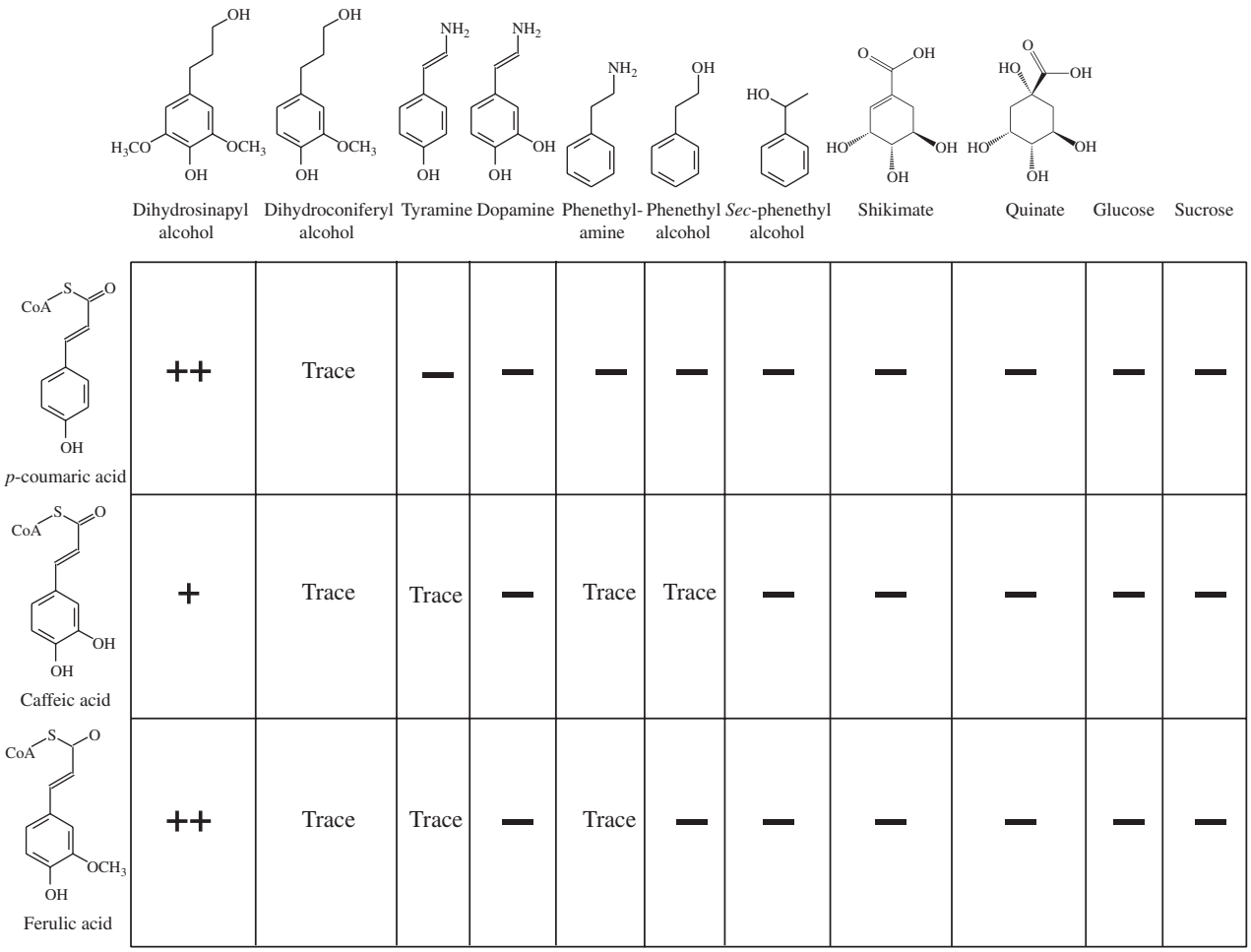

p-coumaric acid	++	Trace	–	–	–	–	–	–	–	–
Caffeic acid	+	Trace	Trace	–	Trace	Trace	–	–	–	–
Ferulic acid	++	Trace	Trace	–	Trace	–	–	–	–	–

Figure 2. Substrate specificity based on conjugate production for purified *p*-coumaroyl CoA:hydroxycinnamyl alcohol transferase in the presence of hydroxycinnamate-CoA donor and non-phenolic acceptor molecules.
++, strong; +, positive (50% of ++); trace, just above threshold of detection; –, not detectable. Conjugate formation was greatest with *p*-coumaroyl CoA or feruloyl CoA as donors and dihydrosinapyl alcohol as acceptor.

were stable and did not show loss of enzyme activity compared to dehydro forms of hydroxycinnamates (Hatfield *et al.*, 2009). HPLC methods showed that transfer of CoA-activated *p*CA, CA or FA to dihydroconiferyl and dihydrosinapyl alcohol was the same as for dehydro forms of the alcohol acceptors (Hatfield *et al.*, 2009). Although the isolated transferase was able to utilize all donor molecules, there was strong preference for *p*-coumaroyl CoA (*p*CA-CoA) or feruloyl CoA (FA-CoA) compared to caffeoyl CoA (50% less). All reactions were performed under identical conditions (substrate concentrations, enzyme amount, pH and temperature), so changes in conjugate formation reflect the ability of the transferase to utilize the donor and acceptor molecules. Acceptor molecules were limited to monolignols with a strong preference for SA. The isolated *p*CAT only produced trace amounts of the *p*CA-CA conjugate *in vitro*, although CA conjugates have been detected in grass lignin (Lu and Ralph, 1999). Compartmentalization may be important for formation of predominantly SA-based conjugates with *p*CA but not with FA, as both FA-CoA and *p*CA-CoA functioned as activated donors in formation of conjugates with dihydrosinapyl alcohol.

Recent work by Withers *et al.* (2012) using a putative *p*CAT gene from rice (Os01g18744.1) expressed in *E. coli* resulted in formation of *p*CA-SA conjugates, but no product formation using FA-CoA. The activity of the *E. coli*-expressed gene was not compared to *in situ* rice *p*CAT activity to determine what percentage of activity the gene product contributed to the whole. Without *in planta* work, it is difficult to interpret how much the putative *p*CAT enzyme from rice contributes to incorporation of *p*CA into rice cell walls.

Determination of pH and temperature optima curves (Methods S1) indicated that the enzyme was most effective at pH 6.5 and a temperature optimum of 40°C using dihydrosinapyl alcohol and *p*CA-CoA as substrates. The enzyme was stable at temperatures of 40°C or less for 3 h of incubation for product formation.

Sequence analysis of trypsin digests of purified transferase protein (performed by the Macromolecular Structure Facility, Michigan State University, East Lansing, MI) provided 12 peptide sequences, with four major sequences (Figure 3). A TBLASTN search (Madden, 2002) of maize sequences identified all four sequences in a single accession, BT042717.1. This sequence is from a 1602 bp mRNA with an unknown function submitted by the Arizona Genomics Institute (full-length cDNA clone ZM_BFc0019F21) corresponding to maize gene GRMZM2G028104. In addition, the identified regions HXXXDG and DFGWG (Figure 3) matched conserved domains that are typically found in BAHD enzymes, families of acyltransferases that utilize CoA thioester activation (D'Auria, 2006), and are consistent with our *p*CAT enzyme.

To determine whether active-site amino acid variations are predictive of apparent substrate specificity differences observed between the maize *p*CAT and rice PMT1 enzyme activities, we performed protein structure homology modeling of the maize *p*CAT and rice PMT1 proteins using SWISS-MODEL (Peitsch, 1995; Arnold *et al.*, 2006; Bordoli *et al.*, 2009; Kiefer *et al.*, 2009). The maize *p*CAT best-fit model was generated using the *Sorghum bicolor* (sorghum) hydroxycinnamoyl CoA:shikimate hydroxycinnamoyl transferase (HCT/HST) crystal structure as a template (Walker *et al.*, 2013) (PDB ID 4ke4_A), whilst the rice PMT1 best-fit model was *coffea* (coffee) hydroxycinnamoyl CoA:quinate hydroxycinnamoyl transferase (HCT/HQT) (Lallemand *et al.*, 2012) (PDB ID 4g2m_A). However, the quality of the global models was deemed low, with QMEAN4 values of 6.81 and 6.59, respectively (Benkert *et al.*, 2011).

The generated models of maize *p*CAT and rice PMT1 were superimposed onto the sorghum HCT/HST structure containing the CoA and *p*CA-shikimate products (Figure S1). The active-site residues are presented. Some key binding and catalytic amino acids identified for HCT/HST are conserved within *p*CAT/PMT1, including Ser38, His162 and Trp386. The models suggest that amino acid deviation between the HCT/HST and *p*CAT/PMT1 proteins may explain the broader hydroxycinnamoyl CoA substrate utilization by *p*CAT/PMT1. For example, several HCT/HST active-site amino acids involved in forming the *p*CA-CoA binding pocket are not perfectly conserved within the *p*CAT/PMT1 proteins. These substitutions include Y40H, M160S, G170A, L171G and M404V. Both the maize *p*CAT and rice PMT1 primary amino acid sequences contain the same changes from the HCT/HST active site amino acids and suggest that other binding site amino acids dictate the hydroxycinnamoyl CoA binding specificity and catalytic differences observed between *p*CAT and PMT1. The nature of the substrate specificity differences between *p*CAT and PMT1 requires future work.

In vivo suppression of *p*CAT gene function in maize

A hairpin RNA interference approach was used for targeted suppression of the maize *p*CAT gene to address the effects of loss of *p*CAT on maize plant development. A cloned cDNA corresponding to the putative maize *p*CAT was obtained (Soderlund *et al.*, 2009) and used to generate pPZP211b-RNAi-*p*CAT (Figure 4a). The pPZP211b-RNAi (Figure 4b) was used as an 'empty vector' control for plant transformations. Both constructs were transformed into immature zygotic embryos of the maize Hi II hybrid genotype by *Agrobacterium*-mediated transformation. Transgenic plants derived from T_1 plants were screened, and positive transgenic *p*CAT-RNAi plants, empty vector-transformed plants and wild-type B73 were used for further analysis.

Real-time PCR analysis of *p*CAT gene suppression

Quantitative real-time PCR was used to determine the extent of *p*CAT gene suppression by the RNAi hairpin transgene. The PCR data suggested that the basal expression level of the *p*CAT gene was low. Expression of GRMZM2G129817, a putative histone acetyltransferase complex component (HATCC), was used for relative quantification. Recent work on gene expression in *Zea mays* had identified a series of genes whose expression did not vary according to plant tissue or developmental stage (Sekhon *et al.*, 2011). HATCC was chosen due to its inherently low but stable level of expression in maize (ranked 28th overall; Sekhon *et al.*, 2011) and the fact that its rice ortholog (Os03 g53960.1) shows similar expression stability in rice (ranked 18th overall; Wang *et al.*, 2010).

Quantitative PCR was performed on cDNA prepared from total RNA isolated from the 7th true leaf tips of a random selection of plants representing *p*CAT-RNAi and empty RNAi transgenic events, as well as from wild-type B73 (Figure 5). The theoretical starting abundance (N_0) for *p*CAT and HATCC transcripts was determined, and used to calculate gene expression ratios for individual plants from

Figure 3. Sequence from *Zea mays* cDNA (ZM_BFc0019F21; GenBank accession number BT042717.1).
Four major peptide sequences from purified protein (underlined/bold) and conserved BAHD domains (boxed) are highlighted. The cDNA encodes the *p*-coumaroyl CoA:hydroxycinnamyl alcohol transferase of maize.

```
      68 MGTIVDADVGFAVKRTSRSLVPPASATPRETLRLSVIDRVAGLR
HLVRSLHVFAAGGDKKRQQATATPAKALREALGKALVDYYPFAGRFVVVDAEGGGETR
VACTGEGAWFVEANAACSLEEARHLDHPMLIPKEQLLPEPSPDVNPLDMPLMMQVTEF
SCGGFVVGLISVHTIADGLGAGQFINTVAAYARGATSATPKPVWARDVIPDPPKMPAP
PPRLDLLLDLRYFTADLSPDHIGKVKARYLESTGQRCSAFDVCVARTWQARVRALRLPD
PAAPVHVCFFANTRHLLPAAATAGFYGNCFYTVKATRASGEVAAADVVDVVRAIRDAK
ARLGADFARWAAGGFDRDPYELTFTYDSLFVSDWTRLGFLEADYGWGTPTHVLPFSYH
PFMAVAVIGAPPKPKPGARIMTMCVQEQHLPEFQEQMMSQQAA 1375
```

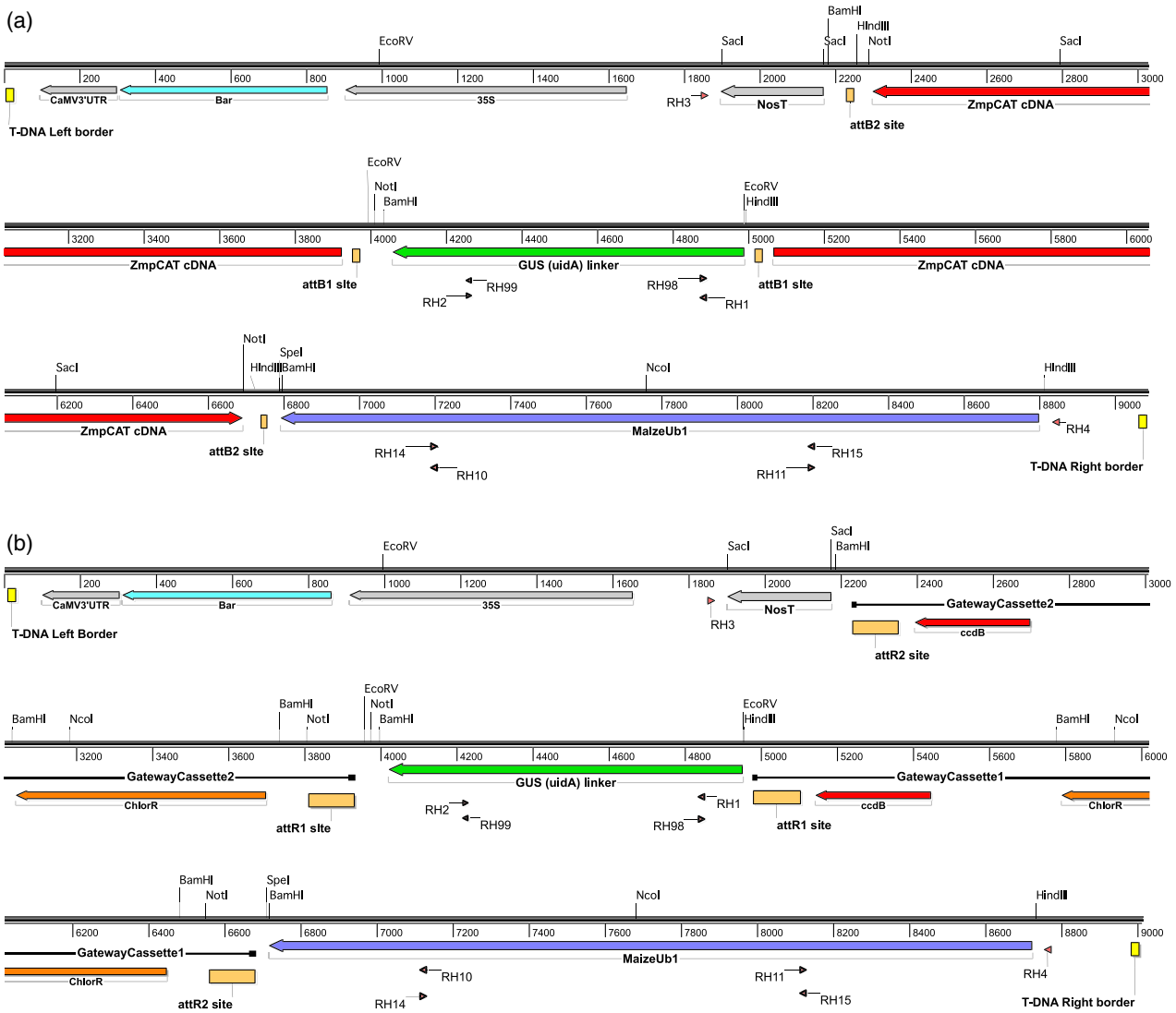

Figure 4. T-DNA maps for RNAi vectors used in maize transformation.
(a) pPZP221b-RNAi-*p*CAT.
(b) pPZP221b-RNAi ('empty vector').
CaMV3′UTR, CaMV 3′ untranslated region/terminator; Bar, glufosinate resistance gene; 35S, CaMV 35S promoter; NosT, nopaline synthase transcriptional terminator; attB and attR sites, Gateway™ recombination sites; Zm*p*CAT cDNA, *Zea mays p*-coumaroyl transferase cDNA, MaizeUb1, maize ubiquitin1 promoter. The Gateway cassettes contain two selection markers: the *ccdB* gene and a chloramphenicol resistance gene (ChlorR). RH numbers indicate the location of the relevant primer. Numbers represent the length in base pairs. Endonuclease restriction sites are indicated above base pairs.

multiple transformation events. Data are grouped based on line background [i.e. *p*CAT-RNAi (prefix 89), pPZP221b-RNAi empty vector (prefix 90) or wild-type (B73)], transformation event (not applicable to wild-type B73), and individual plant number. Amplified products were verified by post-amplification dissociation analysis (Figure S2), with single products of expected thermal characteristics being observed.

Our data indicate plants from several events for which the *p*CAT/HATCC expression ratio is less than that of wild-type B73. Wild-type B73 *p*CAT/HATCC expression ratios ranged from 0.092 to 0.285, with a group mean of 0.185. Based on the microarray data obtained by Sekhon *et al.* (2011), the relative wild-type B73 expression ratio of *p*CAT to HATCC in the leaf tips of the eighth leaf is 0.175 (822.11/4700.49), thus our quantitative PCR results are consistent with previous findings. *p*CAT-RNAi event 10 (89-10) shows the highest and most consistent repression of *p*CAT gene expression, with a group-level mean ratio of 0.020 ± 0.001, indicating that *p*CAT gene expression is 11% of that in wild-type B73. Expression data for other *p*CAT-RNAi events, including 89-6 and 89-13, indicate expression levels of 27% and 42% of wild-type B73, respectively. Empty vector transgenic plants (prefix 90) showed

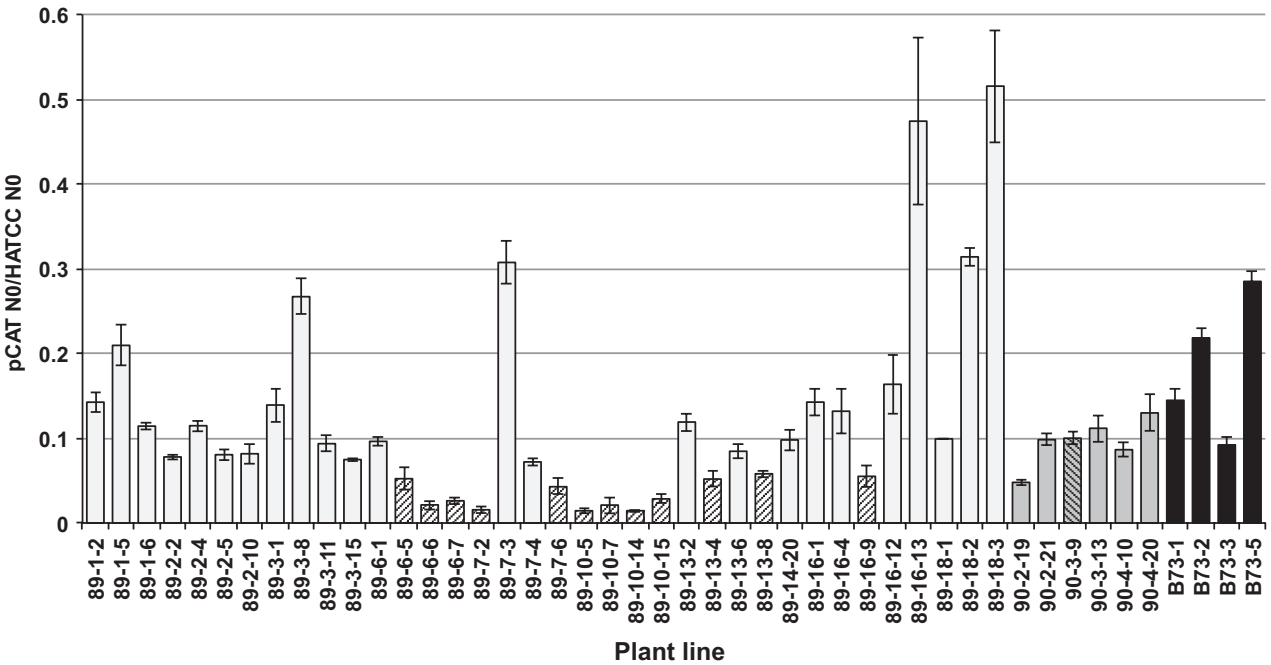

Figure 5. Real-time PCR analysis of *p*CAT gene expression.
The ratio of *p*CAT N_0 to HATCC N_0 for individual maize plants is presented. Candidate *p*CAT-RNAi transgenic plants (prefixed 89; light gray bars) are compared to empty vector plants (prefixed 90; dark gray bars) and wild-type B73 plants (black bars). Error bars represent the SEM. Hatching indicates *p*CAT-RNAi statistically significant gene repression when compared to representative control 90-3-9.

lower mean *p*CAT to HATCC ratios than wild-type (0.096 versus 0.185, respectively). A probable explanation for this difference is the influence of the genetic background of the transgenic plants (Hi II T_0 plants backcrossed to B73) compared to wild-type B73. When strong *p*CAT-RNAi events were compared to empty vector lines, the *p*CAT expression levels were 20.5, 51.1 and 81.7%, respectively, for events 89–10, -6 and -13. These data indicate a range of *p*CAT suppression levels using the *p*CAT-RNAi construct.

To determine whether RNAi-mediated suppression of the maize *p*CAT gene influenced expression of other putative lignin-related genes, we utilized real-time PCR to assess relative expression of candidate genes in control plants (wild-type B73 and empty vector) and *p*CAT-RNAi maize lines. Candidate genes included cinnamyl alcohol dehydrogenase (GRMZM2G090980), caffeic acid 3-*O*-methyltransferase (GRMZM2G082007), caffeoyl CoA 3-*O*-methyltransferase (GRMZM2G127948), ferulate 5-hydroxylase (GRMZM2G 100158), *p*CAT-like (GRMZM2G130728) and putative feruloyl CoA:monolignol feruloyl transferase (GRMZM2 G159641). Selection of genes was based on previous work implying a role in lignin biosynthesis (Penning *et al.*, 2009; Piston *et al.*, 2010; Sekhon *et al.*, 2011; Withers *et al.*, 2012) and expression data from Sekhon *et al.* (2011) demonstrating similar expression profiles to maize *p*CAT.

RNAi-mediated *in vivo* suppression of maize *p*CAT gene expression did not result in compensatory expression of the lignin pathway genes tested (Figure S3). Statistically significant reductions of *p*CAT expression did not correlate with statistically significant altered expression of any of the genes tested. It would be interesting to systematically assess global gene expression variation within pCAT-RNAi plants, but this is beyond the scope of this work.

Impact of suppression of *p*CAT on maize cell walls

Initially, a modified alkaline screening method was used to examine *p*CA levels in leaf blades (4th true leaf) from transgenic *p*CAT-RNAi, empty vector and wild-type B73 maize seedlings. Using this method, plants with reduced *p*CA levels were identified at an early stage of development (Table 1). After grain fill and dry down, mature leaf blade and stem material was harvested from the internode directly above the primary ear attachment to the stem. In all cases, plants with low *p*CA levels in seedlings also had low *p*CA levels in mature material. The *p*CA levels in the mature stems followed a trend similar to that observed in corresponding mature leaf blades. It was concluded that the modified screening method is a reliable means of identifying differences in *p*CA content at an early stage of development and for estimating *p*CA levels in mature plants.

These screening results were used to identify candidate plants for detailed analysis. Ten independent transformation events resulted in plants with some level of *p*CA reduction. The number of plants for each unique transgenic event ranged from 5 to 16 (116 total). Cell walls were

Table 1 Ester-linked *p*CA and FA content (g kg^{-1} cell wall ± SD) in immature and mature plant material from candidate *p*CAT-RNAi transgenic events and empty vector and wild-type B73 controls: mean values for *n* individual plants within independent transgenic events (prefixed 89s), empty vector plants (prefixed 90s) and wild-type inbred B73 plants

		Immature leaves				Mature leaves				Mature stems			
		*p*CA			FA	*p*CA			FA	*p*CA			FA
Event	*n*		High	Low			High	Low			High	Low	
89-1	15	5.97 ± 2.29	10.31	2.21	4.87 ± 0.74	8.73 ± 1.70	11.72	6.31	4.56 ± 0.41	22.10 ± 2.11	26.01	17.48	4.43 ± 0.39
89-2	9	3.21 ± 1.37	6.34	1.62	4.12 ± 0.52	6.72 ± 0.78	7.69	5.26	4.21 ± 0.39	13.57 ± 2.75	16.84	7.76	3.29 ± 0.42
89-3	5	2.93 ± 0.87	3.61	1.47	4.09 ± 0.35	8.07 ± 1.50	9.88	6.47	4.23 ± 0.47	15.66 ± 1.99	17.77	13.03	3.61 ± 0.58
89-6	14	2.21 ± 0.65	3.57	1.37	3.93 ± 0.44	5.37 ± 1.46	8.40	3.26	4.54 ± 0.91	10.82 ± 2.84	14.91	7.11	3.39 ± 0.36
89-7	17	5.18 ± 1.56	9.21	2.82	4.59 ± 0.67	8.20 ± 1.29	10.94	6.45	4.45 ± 0.95	19.00 ± 1.77	23.34	16.01	4.04 ± 0.51
89-10	12	2.26 ± 0.51	3.02	1.68	4.46 ± 0.96	3.72 ± 0.60	4.99	2.69	3.63 ± 0.42	8.10 ± 1.80	12.32	5.82	2.81 ± 0.43
89-13	16	3.41 ± 0.75	4.63	1.97	3.94 ± 0.47	8.03 ± 1.50	9.99	5.42	4.41 ± 0.73	14.11 ± 1.06	15.94	12.94	3.48 ± 0.33
89-14	5	3.24 ± 1.46	5.50	1.83	4.44 ± 0.46	6.67 ± 1.40	7.93	4.41	4.07 ± 0.28	13.44 ± 2.87	16.79	8.95	3.56 ± 0.44
89-16	12	4.91 ± 1.31	7.08	3.06	5.21 ± 0.64	9.29 ± 2.38	14.07	6.53	4.46 ± 0.65	19.02 ± 3.75	24.45	14.49	3.83 ± 0.71
89-18	11	4.33 ± 1.26	6.80	2.55	4.97 ± 0.72	9.46 ± 0.82	10.36	8.12	4.44 ± 0.31	19.63 ± 1.84	23.28	16.13	3.99 ± 0.44
90-	19	5.03 ± 1.66	7.98	2.43	4.22 ± 0.49	11.31 ± 2.58	18.87	7.74	4.31 ± 0.58	22.79 ± 1.52	25.16	19.14	4.07 ± 0.33
B73	5	5.69 ± 0.37	6.08	5.10	5.03 ± 0.61	11.16 ± 2.31	14.27	7.34	4.22 ± 0.79	19.55 ± 1.18	20.91	18.17	4.33 ± 0.32

isolated from candidate transgenic *p*CAT-RNAi, empty vector and wild-type B73 leaf blades and stems. Only the phenolic (ester-linked) and lignin components of the cell walls were analyzed in detail. Figure 6(a) shows the *p*CA levels in mature stems of plants from selected events, including 23 empty vector plants and five B73 control plants. There is variation in *p*CA levels among individual *p*CAT-RNAi plants between specific events resulting from suppression of the *p*CAT gene. The mean *p*CA level for the empty vector group (dashed line) and the mean for the B73 inbred group (solid line) provide reference points to compare individual plants. A summary of gene suppression events, empty vector and B73 controls is given in Table 1 for immature leaves, mature leaves and stems. Mean differences were determined for *p*CAT-RNAi events and those for empty and wild-type B73 vector controls. All transgenic events except one (89-1) were significantly different from empty vector and wild-type B73 controls. Almost all *p*CAT-RNAi lines from events 89-3, 89-6, 89-10 and 89-13 had *p*CA levels that were lower than those of the wild-type B73 and empty vector controls. The pattern of *p*CA reduction in immature compared to mature leaves were the same among transgenic events; the overall levels of *p*CA were higher in the mature leaves as expected: maturation of the plant leads to increased levels of lignin and consequentially increased amounts of *p*CA (Kondo *et al.*, 1990; Chesson *et al.*, 1997; Morrison *et al.*, 1998). Leaf material from independent gene suppression events showed similar patterns to corresponding stem material (Table 1). There did not appear to be a difference in *p*CA incorporation into cell walls between leaves and stems; in other words, transgenic *p*CAT-RNAi plants with lower levels of *p*CA in stems also had lower levels in their leaves.

The amount of FA ester was also measured in each of the plant materials analyzed (Table 1). In this case, only the ester-linked monomer was quantified for each plant, but typically FA monomers are well correlated with total FA in the walls (ester only and ester-plus ether-linked dimers) (Jung and Phillips, 2010; Jung *et al.*, 2011). The significance of the difference between means of *p*CAT-RNAi events and those of empty vector controls was determined. Four transgenic events were significantly different from empty vector and wild-type B73 controls (89-2, 89-6, 89-10 and 89-13). For all transgenic events except 89-10, there was no direct correlation between *p*CAT-RNAi transgenic plants with lower ester-linked *p*CA levels and *p*CAT-RNAi transgenic plants with lower ester-linked FA levels. Three *p*CAT-RNAi events had lines with increased ester-linked FA levels (89-7, 89-14 and 89-16), but these events were not statistically significant compared to empty vector and wild-type B73 controls. No direct correlation existed between *p*CAT-RNAi transgenic plants with higher ester-linked pCA levels and *p*CAT-RNAi transgenic plants with higher ester-linked FA levels. Event 89-10 was an outlier, with 66% of these plants exhibiting lower ester-linked *p*CA and FA compared to empty vector and wild-type B73 controls. This may indicate an influence on FA levels resulting from a positional effect of this particular transgenic event. More detailed analysis beyond the scope of this paper is required to assess whether this is the case. In summary, the cell-wall analyses indicate that incorporation of *p*CA in maize cell walls was affected by targeting the *p*CAT gene. The observed increases and decreases in FA may be associated with this targeted gene, but further studies are required to determine how FA incorporation is affected.

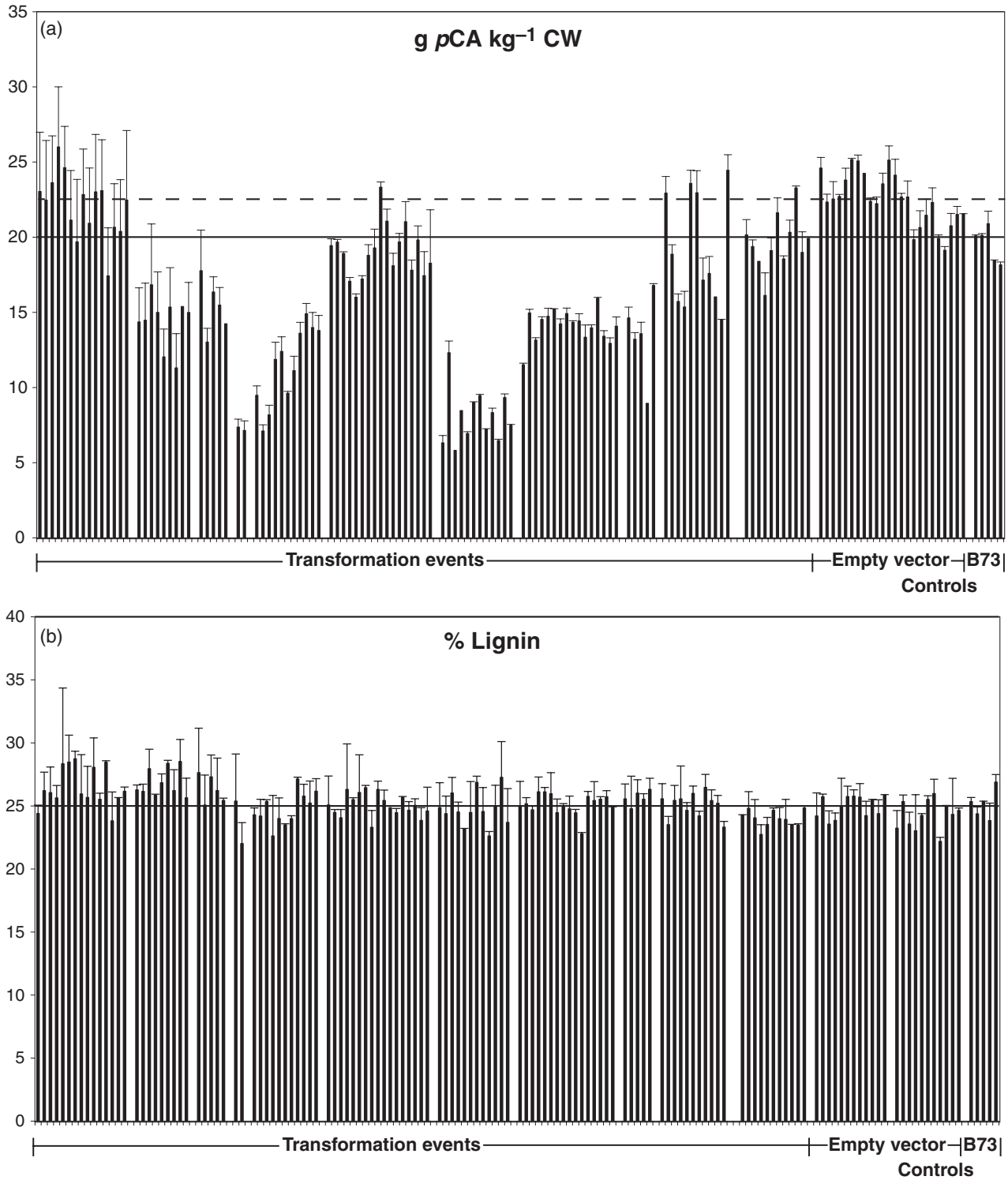

Figure 6. Comparison of (a) *p*-coumarate (*p*CA; g kg^{-1} CW) and (b) lignin (%) in *p*CAT-RNAi lines, empty vector and wild-type B73 controls.
Error bars represent the SEM. Median values for the empty vector (dashed line) and wild-type B73 (solid line) controls are indicated. For lignin, the median values were the same for both control groups.

There are reports in the literature of *p*CA attachment to arabinoxylan or glucuronoarabinoxylan at levels less than for FA (approximately half) (Mueller-Harvey *et al.*, 1986). Incorporation of *p*CA therefore occurs mainly via an ester linkage to monolignols, primarily SA (Lu and Ralph, 1999). It is interesting to note that, in *in vitro* assays, the purified

*p*CAT transferase utilized both FA-CoA and *p*CA-CoA in formation of monolignol conjugates. Addition of FA-CoA only occurred when SA was used as the acceptor molecule. However, structural analysis of lignin (Lu and Ralph, 1999) indicates that this reaction does not occur *in situ*. This suggests possible compartmentalization for the two transferase reactions.

Our original hypothesis was that suppression of *p*CA incorporation into the cell wall would lead to altered lignin amounts and altered composition of lignin if the role of *p*CA is to aid in the formation of lignin, especially S-rich regions (Hatfield *et al.*, 2008a). However, a comparison of the mature stem acetyl bromide lignin values (Figure 6b) with *p*CA levels (Figure 6a) did not support such a role for *p*CA. All events with reduced *p*CA accumulation within the cell walls did not show a reduction in lignin. Testing the significance of the difference between means for individual *p*CAT-RNAi events and empty vector controls identified multiple events (89-2, 89-6, 89-7, 89-10 and 89-13) statistically significant. Event 89-1 had seven out of nine *p*CAT-RNAi plants with increases (1–4%) rather than decreases in lignin values. The reason for the increase in lignin levels in transgenic plants from event 89-1 is not known. In general, the transgenic plants had variable levels of lignin incorporation but no consistent pattern of lignin change (increase or decrease). Even in events where there were more significant reductions in *p*CA (89-6, 89-10 and 89-16), the level of lignin was essentially the same as the empty vector and wild-type B73 controls. This appears to refute the hypothesis that *p*CA incorporation influences the accumulation of lignin.

However, an equally important question was whether the transferase influences the composition of the accumulated lignin. Analysis of the lignin in mature stems using a total cell-wall gel-state 2D NMR technique in deuterated dimethylsulfoxide (DMSO-d_6) (Kim and Ralph, 2010) revealed decreases in incorporation of *p*CA into the cell wall for the *p*CAT-RNAi transgenic plants (Figure 7). Using this approach and focusing on the aromatic regions of the 2D ^{13}C–^{1}H correlation spectra revealed differences in the syringyl:guaiacyl (S:G) distribution in the lignin and other aromatic units in the cell wall. Integration of contours provides S:G integral ratios for 2D NMR spectra (Table 2). The accuracy of quantification of the aromatic unit ratios relies on integrations of well-dispersed 2- and/or 2,6- positions of each aromatic unit. As with most methodologies, more accurate quantification will result from improved NMR methodologies (Lu and Ralph, 2003; Yelle *et al.*, 2008; Kim and Ralph, 2010). The HSQC experiment used here is advantageous because it accounts for all of a given phenolic component within the cell wall (i.e. all G and S units), whereas other techniques such as thioacidolysis, derivatization followed by reductive cleavage, and nitrobenzene oxidation only release those units ether-linked to other components. This provides a holistic view of the lignin/phenolic region of the cell wall, allowing easy comparison of the various phenolic components and lignin subunits. In those events with modest decreases in *p*CA (e.g. 89-18; 11.8 and 19.1 g kg^{-1} CW (cell wall), respectively) compared to empty vector or wild-type B73 controls (22.5 and 20.1 g kg^{-1} CW, respectively), there was a similar decrease in S units in the corresponding lignin based on S:G ratios (Table 2). It was difficult to judge the precise extent of reduction due to the relatively small changes and the NMR signals associated with them. Larger reductions in *p*CA incorporation into the wall, such as seen in event 89-10 (67% reduction), led to significantly lower S unit content in the lignin (Table 2). One explanation may be that the maize plant has mechanisms to compensate for lignin component changes in order to maintain an optimum or threshold level of total lignin irrespective of the monolignol composition within the cell wall. In this case, the lignin monomer pathway shifts to incorporate more G units. These results indicate that suppression of *p*CAT in maize alters the composition of its lignin by decreasing formation of the *p*CA-SA conjugate. Lower conjugate formation decreases the amount of SA incorporated, resulting in lower S content in the lignin. The overall decrease in SA incorporation is dependent on the level of transferase expression.

CONCLUSIONS

Purification of the *p*-coumaroyl transferase activity from maize stems followed by peptide analysis led to identification of a *p*-coumaroyl CoA:hydroxycinnamyl alcohol transferase gene in maize. Suppression of the *p*CAT gene in maize resulted in decreased incorporation of *p*CA into the cell walls. Together with this reduction in *p*CA, there was also a reduction in SA incorporation into the cell wall but not a decrease in the total lignin content. It is clear that *p*CAT aids in incorporation of SA into growing lignin polymers; however, regulation of *p*CAT gene expression does not appear to control the total amount of lignin within the cell wall.

The biological significance of regulating *p*CAT gene expression in maize is not known. We are continuing to research the effects of *p*CAT gene suppression in maize through developmental studies and *in vitro*/*in vivo* digestibility studies.

EXPERIMENTAL PROCEDURES

Protein purification of transferase

Plant material. Maize inbred line B73 was grown at the US Dairy Forage Research Center, Madison, WI. Plants were harvested at the 7th internode (just above the soil line) at tassel emergence. Leaves and sheaths were excised from stems, and rind and pith

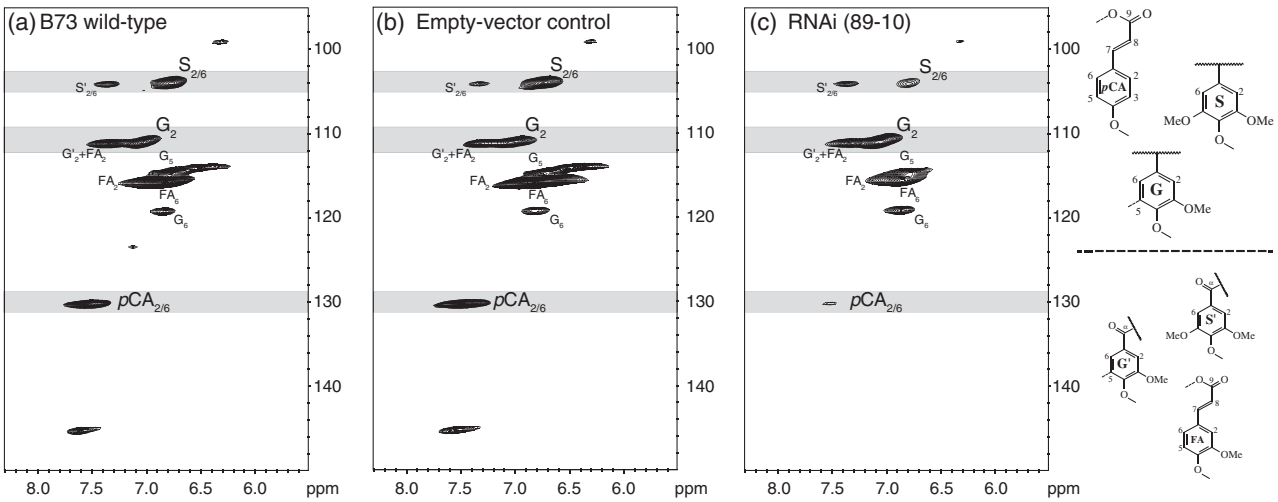

Figure 7. Aromatic regions of gel-state 2D-NMR spectra in DMSO-d_6. 2D ^{13}C-^{1}H HSQC correlation spectra from stem cell walls of
(a) B73 wild-type,
(b) the empty vector control, and
(c) a representative *p*CAT-RNAi line (89-10) are shown. Correlations from the aromatic rings represent unique types of aromatic units (syringyl $S_{2/6}$, guaiacyl G_2 and *p*-coumarates $pCA_{2/6}$). Assignments are based on model compound data in the NMR database of lignin and cell wall model compounds (Ralph *et al.*, 1993).

Table 2 Lignin composition in mature leaves and stems from candidate *p*CAT-RNAi transgenic plants (prefixed 89) compared to empty vector plants (prefixed 90) and wild-type B73 controls

	Leaf		Stem	
Event	S:G	S:*p*CA	S:G	S:*p*CA
89-6-16	0.32	1.48	0.41	0.98
89-10-2	0.25	1.92	0.35	2.44
89-18-2	0.36	1.76	0.54	0.80
90-6-14	0.40	1.72	0.63	0.91
B73-3	0.40	2.03	0.61	1.04

Values are integral ratios based on integration of contours [syringyl ($S_{2/6}$), guaiacyl (G_2) and *p*-coumarate ($pCA_{2/6}$)] from gel-state 2D NMR spectra.

were separated, with only rind being used for further analyses (Hatfield *et al.*, 2008b). Rind tissues were pooled, homogenized using a Robot Coupe (Robot Coupe, Ridgeland, MS, USA) model R2UB (serrated S blade), frozen in liquid nitrogen and stored at −80°C.

Buffers. The buffers used in purification of the transferase were (A) 50 mM MOPS containing 5% v/v glycerol, pH 7.5, (B) 25 mM MOPS, pH 7.5, (C) 25 mM MOPS containing 1 M KCl, pH 7.5, (D) 25 mM MOPS containing 30% w/v $(NH_4)_2SO_4$, pH 7.5, (E) 50 mM MOPS containing 150 mM CH_3CO_2Na, pH 7.5, (F) 10 mM Tris, pH 7.5, and (G) 10 mM Tris containing 1 M KCl, pH 7.5.

Chromatographic purification scheme. The steps were performed on ice or at 4°C and used the Bio-Rad Biologic DuoFlow system (Bio-Rad, Hercules, CA, USA).

Maize extraction—Extraction of *p*CAT activity was performed as previously described (Hatfield *et al.*, 2008b). Briefly, frozen samples were ground in liquid nitrogen, weighed into a beaker, and 2 ml per g fresh tissue of buffer A was added with 4 μl ml^{-1} protease inhibitor (Sigma, product code P9599; Sigma-Aldrich, St. Louis, MO, USA). The slurry was stirred on ice (2 h) and filtered through two layers of Miracloth (EMD Millipore, Billerica, MA, USA) before clarifying by centrifugation (22 000 ***g*** for 20 min). The supernatant was collected, frozen in liquid nitrogen and stored at −80°C.

Ammonium sulfate precipitation—Frozen maize extract (approximately 350 ml) was thawed and stirred for 20–25 min in a beaker on ice containing ammonium sulfate (65% saturation). The precipitated protein was pelleted at 22 000 ***g*** for 20 min (5°C). Protein pellets were dissolved in buffer B and concentrated to approximately 15 ml by ultrafiltration under nitrogen (YM10 UF membrane, EMD Millipore).

DEAE 650M anion-exchange column—The partially purified protein was applied to a DEAE 650M anion-exchange column (length 15 cm, internal diameter 2.5 cm; Toyopearl™; Tosoh Bioscience LLC, King of Prussia, PA, USA)) equilibrated in buffer B. The column was washed with buffer B (50 ml) before applying a gradient of 0–50% buffer C (110 ml) followed by 50–100% buffer C (40 ml) at a constant flow (1 ml min^{-1}). Active fractions were pooled and concentrated by ultrafiltration under nitrogen (345 kPa, YM30 UF membrane, EMD Millipore) with buffer exchanged to buffer B.

Butyl sepharose hydrophobic interaction column—Ammonium sulfate was added to partially purified protein from the preceding step to 30% saturation, and mixed on ice (20–30 min). The sample was clarified by centrifugation at 22 400 ***g*** for 20 min before applying to a butyl Sepharose column (length 15 cm, internal diameter 1 cm) equilibrated in buffer D. The column was washed using 10 ml of buffer D, and active fractions were eluted using a gradient of buffer B (0–50% for 30 ml; then 50–100% for 30 ml) at a constant flow (1.25 ml min^{-1}). Active fractions were pooled and concentrated to <1 ml using a Centricon Ultra-15 filter (Amicon; EMD Millipore) with buffer exchanged to buffer E.

S100 size-exclusion column—Partially purified protein from the preceding step was applied to a S100 column in buffer E, and eluted at 0.65 ml min^{-1} for 180 ml. Active fractions were pooled, dialyzed against 300 ml buffer F and concentrated to 0.45 ml using a Centricon Ultra-15 filter (Amicon).

Reactive yellow 3 affinity column—The concentrated protein from the preceding step was applied to a Reactive Yellow 3–agarose column (5 × 25 mm, width × length; Sigma-Aldrich) equilibrated with buffer F. Column flow was stopped 25 min after protein addition to allow active fractions to bind. The column was washed using 10 ml buffer F, incubated with 0.5 ml of 10 mM *p*CACoA for 25 min, and then eluted with 10 ml buffer F. The flow (0.25 ml min^{-1}) was constant, and active fractions were pooled and concentrated to approximately 1 ml using a Centricon Ultra-15 filter (Amicon).

Bio-Rad UNO Q1R anion-exchange column—Purified protein from the preceding step was applied to an UNO Q1R (Bio-Rad) anion-exchange column (1.7 × 35 mm, width × length; in buffer F) and washed using 10 ml buffer F. Active fractions were eluted with a gradient of buffer G (0–15% buffer G for 30 ml; hold at 15% buffer G for 5 ml; then 15–25% buffer G for 10 ml; hold at 25% buffer G for 5 ml) at a constant flow (0.75 ml min^{-1}). Active fractions were pooled, concentrated using a Centricon Ultra-15 filter (Amicon) and stored at -80°C.

Synthesis of CoA thioester substrates. Preparation of thioesters was performed as previously described (Hatfield *et al.*, 2009).

Substrate specificity for pCAT enzyme activity. Pairwise combinations of acyl donor (*p*CA-CoA, FA-CoA, CA-CoA and acetyl CoA) and acyl acceptor (dihydrosinapyl alcohol, dihydroconiferyl alcohol, tyramine, dopamine, sec-phenethyl alcohol, phenethyl alcohol, phenethylamine, shikimate, quinate, glucose and sucrose) were evaluated in transferase assays using purified transferase protein. Product recovery and quantification were performed as previously described (Hatfield *et al.*, 2009).

Protein structure homology-modeling. Predicted amino acid sequences for the maize *p*CAT and rice PMT1 proteins were subjected to alignment-mode protein structure homology modeling using SWISS-MODEL (Peitsch, 1995; Arnold *et al.*, 2006; Bordoli *et al.*, 2009; Kiefer *et al.*, 2009; Benkert *et al.*, 2011). Best-fit models were superimposed onto the sorghum hydroxycinnamoyl CoA: shikimate hydroxycinnamoyl transferase (HCT/HST) crystal structure (Walker *et al.*, 2013) (PDB ID 4ke4_A) with bound CoA and *p*CA-shikimate, and visualized using DeepView software (Guex and Peitsch, 1997).

Trypsin digest and peptide sequencing. Purified protein associated with the *p*-coumaroyl CoA:hydroxycinnamyl alcohol transferase was subjected to trypsin digestion followed by peptide sequence analysis by MS/MS at the Macromolecular Structural Facility (Michigan State University, East Lansing, MI), according to their standard procedures.

Gene analysis of *p*CAT

DNA primers and associated materials. All DNA primers (Table 3) were synthesized by the DNA Synthesis Facility of the Biotechnology Center of the University of Wisconsin Madison. All DNA sequencing was performed using ABI BigDye™ Terminator reagents and Agencourt™ CleanSEQ™ (Beckman Coulter, Inc., Indianapolis, IN, USA) magnetic bead clean-up, and analyzed at the DNA Sequencing Facility of the Biotechnology Center of the University of Wisconsin Madison.

pCAT cDNA. A cDNA clone (ZM_BFc0019F21; GenBank accession number BT042717.1) encoding the putative *Zea mays p*CAT (GRMZM2 g028104) was obtained from the University of Arizona, Department of Plant Sciences, Arizona Genomics Institute (Soderlund *et al.*, 2009). To facilitate subsequent LR recombination reactions, the *p*CAT cDNA was moved from pCMVSport6.1-*Zmp*CAT to pDONR221 by a BP recombinase reaction (Invitrogen/Life Technologies, Grand Island, NY, USA). The pDONR221-*p*CAT plasmid product was verified by DNA sequencing using primers RH8 and RH9 (Table 3).

In planta *RNAi vector construction.* A modified, Gateway cloning-compatible *in planta* RNAi vector was constructed based on the expression cassette for the pANDA series of monocot RNAi vectors (Miki and Shimamoto, 2004; Miki *et al.*, 2005). The pANDA mini vector was obtained from Hiroyuki Tsuji (Nara Institute of Science and Technology, Nara, Japan), and used as a source for the *Ub1* promoter-driven Gateway-compatible cloning RNAi construct. Two restriction digest fragments from the pANDA mini vector were obtained inseries and cloned sequentially into pPZP221b (Hajdukiewicz *et al.*, 1994; Kang *et al.*, 2001). First, an approximately 4.5 kb *Spe*I fragment from the pANDA mini vector containing both Gateway cassettes and the GUS linker was cloned into the *Xba*I site of the binary vector, and the orientation of resulting product was verified by restriction digest with *Hin*dIII. Second, an approximately 3.7 kb *Hin*dIII fragment from the pANDA mini vector (containing the *Ub1* promoter and the first Gateway cassette) was cloned into the *Spe*I fragment-containing, *Hin*dIII-digested binary vector. Plasmids from the resulting clones were analyzed by colony PCR using primers RH4 and RH11, and *Nhe*I restriction enzyme digests, and verified by DNA sequencing using primers RH1, RH2, RH3, RH4 and RH10. Finally, a Nos transcriptional terminator flanked by *Sac*I sites was PCR-amplified using Phusion high-fidelity DNA polymerase (Finnzymes/Thermo Fisher Scientific Inc., Waltham, MA, USA) using primers RH104 and RH105. The purified PCR product was digested with *Sac*I and ligated directionally into the binary vector multiple cloning site *Sac*I site. The resulting clones were screened for ligation directionality using colony PCR with primers RH6 and RH105. DNA sequencing using primers RH3, RH4, RH98 and RH99 was used to verify the sequence of the resulting vector (pPZP211b-RNAi).

To generate the pPZP221b-*p*CAT-RNAi vector for gene activity suppression, the binary pPZP211b-RNAi vector and the pDONR221-*p*CAT cDNA vector were recombined using LR recombinase (Invitrogen/Life Technologies). The vector product, pPZP211b-RNAi-*p*CAT (*p*CAT-RNAi), was analyzed by restriction digestion and verified by DNA sequencing using primers RH3, RH4, RH98 and RH99 to assess vector–insert junctions.

Maize plant transformation and selection. Transgenic maize lines were generated by *Agrobacterium*-mediated transformation of either *p*CAT-RNAi or pPZP211b-RNAi at the Plant Transformation Facility at Iowa State University (http://agron-www.agron.iastate.edu/ptf/) using their standard procedures. The maize Hi II cultivar was used to generate glufosinate-resistant T_0 plants, which were crossed to maize B73 resulting in the T_1 seed received from the Plant Transformation Facility at Iowa State University. T_1-

Table 3 DNA oligos: laboratory identification number (ID), common name, nucleotide sequence with underlined added restriction sites, and purpose

ID	Name	Sequence	Purpose
RH1	GUS-linker 1	5′-catgaagatgcggacttacg-3′	Amplify GUS linker in pANDA series
RH2	GUS-linker 2	atccacgccgtattcgg	Amplify GUS linker in pANDA series
RH3	SB496 (M13rev overlap)	gagcggataacaatttcacacag	Colony PCR, DNA seq. binaries
RH5	Gateway cassette 1 (GL19)	cacattatacgagccggaagcat	DNA sequencing
RH6	Gateway cassette 2 (GL20)	cagtgtgccggtctccgttatcg	Colony PCR, DNA sequencing
RH8	M13For-20	gtaaaacgacggccag	Colony PCR, DNA sequencing
RH9	M13rev	caggaaacagctatga	Colony PCR, DNA sequencing
RH10	3′ out UbPromoter	cgttcattcgttctagatcgg	DNA sequencing
RH12	5′ pANDA cassette (FspI)	tgcgcaagtgcagcgtgacccg	PCR amplification, pANDA cassette (*Fsp*I)
RH13	3′ pANDA cassette (FspI)	atgcgcaattcccgatctagtaacatag	PCR amplification, pANDA cassette (*Fsp*I)
RH14	RH10 comp	ccgatctagaacgaatgaacg	DNA sequencing
RH15	RH11 comp	cgacgagtctaacggacacc	DNA sequencing
RH98	Revcomp RH1	cgtaagtccgcatcttcatg	Colony PCR, DNA sequencing
RH99	Revcomp RH2	ccgaatacggcgtggat	Colony PCR, DNA sequencing
RH104	5′ SacI-NosT	agagctcgaatttccccgatcgttcaaac	PCR amplification, Nos terminator
RH105	3′ SacI-NosT	agagctcccgatctagtaacatagatgacacc	PCR amplification, Nos terminator
RH131	HATCC_F[a]	agggactttgctgttacctggag	Real-time PCR
RH132	HATCC_R[a]	caagtgcatcttccaccttgacc	Real-time PCR
RH227	*p*CAT forward	acacattccatcggtcgtgaa	Real-time PCR
RH228	*p*CAT reverse	gacgatggtgcccatagctaa	Real-time PCR
JMM26	Maize actin[b]	gaagttccgggatctgaag	Genomic marker, genomic DNA prep quality
JMM27	Maize actin[b]	ctcgtggacgatgtggtta	Genomic marker, genomic DNA prep quality

[a]HATCC_F or R, FRMZM2G129817.
[b]Maize actin-depolymerizing factor 2 (ADF), GRMZM2G097122.

derived plants were selected using two methods: PCR and glufosinate resistance. Genomic DNA was isolated from leaf tips based on procedures adapted from Wang *et al.* (2005). PCR was performed using primers specific to the GUS linker of the RNAi transgene (RH1 and RH2) or targeting GRMZM2G097122 encoding actin-depolymerizing factor 2 (JMM26 and JMM27), a generic genomic DNA marker used to verify genomic DNA preparation quality. To corroborate PCR results, resistance to Ignite herbicide (24.5% by weight; active ingredient glufosinate ammonium; Bayer CropScience, Research Triangle Park, NC, USA) was assessed by spraying with 250 mg l^{-1} Ignite, and repeating the application 3 days later. Yellowing/death of non-transgenic plants was recorded 1 week after spraying.

Plant RNA isolation, cDNA synthesis, and quantitative real-time PCR analysis. DNA-free total RNA from the 7th true leaf (before complete leaf expansion) was isolated from frozen and ground tissue using a Spectrum™ plant total RNA kit (protocol A; Sigma). First-strand cDNA synthesis was performed using the GoScript™ reverse transcription system (Promega, Madison, WI, USA) and a polyT primer. One microgram of total RNA was used for the cDNA synthesis reactions. The cDNA was used for quantitative real-time PCR using SYBR Green master mix (Thermo Fischer Scientific); PCR was performed essentially as described previously (Sullivan, 2009). Primer design for *p*CAT was performed using Primer Express 2 software (Thermo Fischer Scientific) with default parameters, resulting in 5′ UTR-specific primers RH227 and RH228, of which RH227 complimentary sequence was not present in the cDNA used for pPZP211b-RNAi-*p*CAT (DR102) construction but was contained in the endogenous transcript. Primer design for the control gene encoding HATCC (histone acetyltransferase complex component; GRMZM2 g129817) was performed using the web-based QuantPrime qPCR primer design software (http://www.quantprime.de) (Arvidsson *et al.*, 2008) with default parameters, resulting in exon-spanning primers RH131 and RH132. Reactions were performed using an ABI 7300 real-time PCR system (Thermo Fischer Scientific) under the following conditions: 10 min denaturation at 95°C, 45 cycles of 95°C for 10 sec and 58°C for 1.5 min, followed by amplification product dissociation analysis. Real-time PCR data were analyzed using the LinRegPCR method (Ramakers *et al.*, 2003; http://www.hartfaalcentrum.nl/index.php?main=files&sub=LinRegPCR). N_0 values for individual reactions run in triplicate were determined, and arithmetic means were used to calculate mean relative leaf-tip expression ratios of *p*CAT to HATCC for individual plants. ANOVA statistical analysis with Dunnett's *post hoc* test ($\alpha = 0.05$; control line 90-3-9) was performed using Prism 5 (GraphPad Software Inc., http://www.graphpad.com/company/).

Real-time PCR analysis for genes associated with lignin biosynthesis was performed essentially as described above. Real-time PCR primers (Table S1) were designed for genes encoding putative enzymes including a cinnamyl alcohol dehydrogenase, a caffeoyl CoA 3-*O*-methlytransferase, a ferulate 5-hydroxylase and a putative feruloyl CoA:monolignol feruloyl transferase using QuantPrime qPCR primer design software (Arvidsson *et al.*, 2008). Primers for genes encoding *p*CAT-like and caffeic acid 3-*O*-methyltransferase enzymes were designed using Primer BLAST software (Ye *et al.*, 2012).

Cell-wall analysis

Plant materials. Maize seeds acquired from the Plant Transformation Facility at Iowa State University were germinated in 15 cm pots. Plants were allowed to reach the 4th true leaf stage before genomic DNA isolation/PCR genotyping and spraying with

Ignite to remove non-transgenic plants. Plants were then transplanted to 11.4 L pots, watered as required to maintain adequate soil moisture, and fertilized weekly using a soluble fertilizer (nitrogen-phosphorus-potassium 10-10-10; 5 g per pot). The 4th true leaf was harvested, and tissue-dried at 55°C for alkaline screening (see below). Mature leaf and stem material was harvested and immediately frozen in liquid nitrogen before grinding in a freezer mill and storage at −80°C for further analysis. The cell walls of the ground mature leaves and stems were processed for analysis of lignin and cell-wall phenolics, and prepped for NMR analysis.

Modified maize alkaline screening method. The dried 4th true leaf was ground to 1 mm using a UDY mill (Udy Corp, Fort Collins, CO, USA), and further processed using a bead-beater mill (5000 rpm for 10 sec using one 4 mm glass bead; Cole-Parmer, Vernon Hills, IL, USA). Alkaline extraction of phenolics was performed based on the Jung and Phillips method (Jung and Phillips, 2010). Essentially, ground material (approximately 15 mg) was incubated for 20–24 h at 39°C in 2 N NaOH with 2-mercaptoethanol. HCl (6 M) was added to bring the pH to <2.0, and samples were incubated for 2 h at 4°C. Samples were centrifuged at 15 300 ***g*** for 5 min, and supernatants were passed through prepared C18 columns (ENVI-18; Sigma-Aldrich). Phenolics were eluted using MeOH and verified by HPLC on a Gemini 5 μm C6 phenyl column (Phenomenex, Torrance, CA, USA, 110 Å, 4.6 × 250 mm; width × length). The HPLC was performed at a flow rate of 1 ml min^{-1} using solvent A (>99% HPLC-grade MeOH and 0.0125% trifluoroacetic acid) and solvent B (>99% ultra-pure dH_2O and 0.0125% TFA). The HPLC method was as follows: 5 min at 20% solvent A, 10 min at 65% solvent A, then 6 min at 10% solvent B, followed by 7 min at 20% solvent A to re-equilibrate. Standards of FA and *p*CA were used to verify phenolic products.

Lignin determination of grass stems. Isolated cell-wall samples (approximately 20 mg) were analyzed for lignin using the acetyl bromide method as modified by Hatfield *et al.* (1999a). The extinction coefficient (17.75 cm^2 g^{-1}) used to determine lignin concentration was based on that of a purified HCl-dioxane lignin isolated from maize stems (Fukushima and Hatfield, 2001). The lignin composition was examined by 2D NMR as described by Kim *et al.* (2008) (see below).

Cell-wall phenolics in grass stems. Cell walls (20 mg) were analyzed for ester-linked phenolics as described by Grabber *et al.* (1995). Phenolics were identified and quantified as trimethylsilane derivatives [40 μl N-trimethylsilylimidazole (Pierce) and 10 μl pyridine] using gas liquid chromatography - flame ionization detector (GLC-FID) on a ZB-5 ms column (Zebron; 30 m × 0.25 mm, 0.25 μm). The GLC conditions were: injector 315°C, detector 300°C, and a temperature program of 200°C for 1 min, increasing by 4°C per min to 248°C, then 30°C per min to 300°C, and holding for 20 min. GLC conditions were run at a constant pressure of 124 kPa. Standards of FA and *p*CA were used to verify phenolic products.

NMR sample preparation. Gel-state NMR cell-wall samples were prepared using a method similar to that described by Kim *et al.* (2008). Essentially, cell walls (70 mg) were transferred into 5 mm NMR tubes after ball-milling. A 4:1 mixture of DMSO-d_6 and pyridine-d_5 (0.5 ml) was carefully added to each NMR tube. NMR tubes were capped and placed in a sonicator for 2–4 h until the sample was evenly wet and a gel matrix had formed.

NMR experiments. NMR experiments were performed using a 500 MHz (DRX-500) Bruker Biospin instrument (Bruker, Billerica, MA, USA), equipped with an inverse gradient 5 mm TXI $^1H/^{13}C/^{15}N$ cryoprobe. The central DMSO solvent peak was used as the reference peak (δ_C 39.5, δ_H 2.49). An adiabatic HSQC experiment (hsqcetgpsisp) (Kupce and Freeman, 2007) was performed, with the following parameters: 32 transient spectral increments were acquired from 10 to 0 ppm in F2 (^1H) using 1000 data points, from 200 to 0 ppm in F1 (^{13}C) using 320 data points of 776 NS (F1 acquisition time 6.3 msec), with a total acquisition time of 24 h 19.2 min. Processing used matched Gaussian apodization in F2 and a squared cosine bell in F1. Integration of contours was done using Bruker Topspin version 3.1 software (http://www.bruker.com/).

Statistical analysis

All the experiments were independently performed in duplicate for all measurements. The means were analyzed, and statistical differences were determined using one-way analysis of variance followed by multiple comparison tests ($\alpha = 0.05$ and $\alpha = 0.01$). The standard error was calculated using *n* values of each experiment.

FOOTNOTE

During the review process for our paper, it came to our attention that a similar paper was to be published. That paper dealt with characterization of plants mis-expressing a Brachypodium *p*CA transferase Petrik *et al.* (2014) ortholog in the model grass *Brachypodium distachyon*. Our work directly tests the role of *p*CA transferase in the economically important plant *Zea mays* L. The results from the two studies complement each other.

ACKNOWLEDGEMENTS

The authors are indebted to laboratory assistants Lindsay Stafslien, Corinna Ranweiler, Rebecca McGuire, Justin Marita and Emily Phillips for their help over the duration of the project. Mention of a trademark or proprietary product does not constitute a guarantee or warranty of product by the US Department of Agriculture, nor does it imply approval to the exclusion of other suitable products.

SUPPORTING INFORMATION

Additional Supporting Information may be found in the online version of this article.

Figure S1. Protein homology modeling of maize *p*CAT and rice PMT1 active-site amino acids to the sorghum HCT1 X-ray crystal structure.

Figure S2. Thermal dissociation analysis of the *p*CAT and HATCC quantitative RT-PCR products.

Figure S3. Real-time PCR gene expression analysis of lignin-related genes in selected *p*CAT-RNAi and control maize lines.

Table S1. Lignin related RT-PCR oligos and uses.

Methods S1. Methods for determination of *p*CAT enzyme activity temperature and pH optima.

REFERENCES

Arnold, K., Bordoli, L., Kopp, J. and Schwede, T. (2006) The SWISS-MODEL workspace: a web-based environment for protein structure homology modelling. *Bioinformatics*, **22**, 195–201.

Arvidsson, S., Kwasniewski, M., Riano-Pachon, D. and Mueller-Roeber, B. (2008) QuantPrime – a flexible tool for reliable high-throughput primer design for quantitative PCR. *BMC Bioinformatics*, **9**, 465.

Back, K., Jang, S.M., Lee, B.C., Schmidt, A., Strack, D. and Kim, K.M. (2001) Cloning and characterization of a hydroxycinnamoyl CoA:tyramine N–(hydroxycinnamoyl)transferase induced in response to UV–C and wounding from *Capsicum annuum*. *Plant Cell Physiol.* **42**, 475–481.

Benkert, P., Biasini, M. and Schwede, T. (2011) Toward the estimation of the absolute quality of individual protein structure models. *Bioinformatics*, **27**, 343–350.

Bordoli, L., Kiefer, F., Arnold, K., Benkert, P., Battey, J. and Schwede, T. (2009) Protein structure homology modeling using SWISS-MODEL workspace. *Nat. Protoc.* **4**, 1–13.

Chesson, A., Provan, G.J., Russell, W., Scobbie, L., Chabbert, B. and Monties, B. (1997) Characterisation of lignin from parenchyma and sclerenchyma cell walls of the maize internode. *J. Sci. Food Agric.* **73**, 10–16.

D'Auria, J.C. (2006) Acyltransferases in plants: a good time to be BAHD. *Curr. Opin. Plant Biol.* **9**, 331–340.

D'Auria, J.C., Pichersky, E., Schaub, A., Hansel, A. and Gershenzon, J. (2007) Characterization of a BAHD acyltransferase responsible for producing the green leaf volatile (Z)–3–hexen-1–yl acetate in *Arabidopsis thaliana*. *Plant J.* **49**, 194–207.

Ford, C.W. and Hartley, R.D. (1989) GC/MS characterization of cyclodimers from *p*–coumaric and ferulic acids by photodimerization – a possible factor influencing cell wall biodegradability. *J. Sci. Food Agric.* **46**, 301–310.

Ford, C.W. and Hartley, R.D. (1990) Cyclodimers of *p*–coumaric and ferulic acids in the cell walls of tropical grasses. *J. Sci. Food Agric.* **50**, 29–43.

Fukushima, R.S. and Hatfield, R.D. (2001) Extraction and isolation of lignin for utilization as a standard to determine lignin concentration using the acetyl bromide spectrophotometric method. *J. Agric. Food Chem.* **49**, 3133–3139.

Grabber, J.H., Hatfield, R.D., Ralph, J., Zon, J. and Amrhein, N. (1995) Ferulate cross-linking in cell-walls isolated from maize cell-suspensions. *Phytochemistry*, **40**, 1077–1082.

Guex, N. and Peitsch, M.C. (1997) SWISS-MODEL and the Swiss-PdbViewer: an environment for comparative protein modeling. *Electrophoresis*, **18**, 2714–2723.

Hajdukiewicz, P., Svab, Z. and Maliga, P. (1994) The small, versatile pPZP family of *Agrobacterium* binary vectors for plant transformation. *Plant Mol. Biol.* **25**, 989–994.

Harris, P.J. and Hartley, R.D. (1980) Phenolic constituents of the cell walls of monocotyledons. *Biochem. Syst. Ecol.* **8**, 153–160.

Hatfield, R.D., Grabber, J.H., Ralph, J. and Brei, K. (1999a) Using the acetyl bromide assay to determine lignin concentrations in herbaceous plants: some cautionary notes. *J. Agric. Food Chem.* **47**, 628–632.

Hatfield, R.D., Ralph, J. and Grabber, J.H. (1999b) Cell wall cross-linking by ferulates and diferulates in grasses. *J. Sci. Food Agric.* **79**, 403–407.

Hatfield, R., Ralph, J. and Grabber, J.H. (2008a) A potential role for sinapyl *p*–coumarate as a radical transfer mechanism in grass lignin formation. *Planta*, **228**, 919–928.

Hatfield, R.D., Marita, J.M. and Frost, K. (2008b) Characterization of *p*–coumarate accumulation, *p*–coumaroyl transferase, and cell wall changes during the development of corn stems. *J. Sci. Food Agric.* **88**, 2529–2537.

Hatfield, R.D., Marita, J.M., Frost, K., Grabber, J., Ralph, J., Lu, F.C. and Kim, H. (2009) Grass lignin acylation: *p*–coumaroyl transferase activity and cell wall characteristics of C3 and C4 grasses. *Planta*, **229**, 1253–1267.

Jung, H.G. and Casler, M.D. (1991) Relationship of lignin and esterified phenolics to fermentation of smooth bromegrass fibre. *Anim. Feed Sci. Technol.* **32**, 63–68.

Jung, H.G. and Phillips, R.L. (2010) Putative seedling ferulate ester (*sfe*) maize mutant: morphology, biomass yield, and stover cell wall composition and rumen degradability. *Crop Sci.* **50**, 403–418.

Jung, H.G., Mertens, D.R. and Phillips, R.L. (2011) Effect of ferulate-mediated lignin/arabinoxylan cross-linking in corn silage on feed intake, digestibility, and milk production. *J. Dairy Sci.* **94**, 5124–5137.

Kang, B.H., Busse, J.S., Dickey, C., Rancour, D.M. and Bednarek, S.Y. (2001) The Arabidopsis cell plate-associated dynamin-like protein, ADL1Ap, is required for multiple stages of plant growth and development. *Plant Physiol.* **126**, 47–68.

Kiefer, F., Arnold, K., Kunzli, M., Bordoli, L. and Schwede, T. (2009) The SWISS-MODEL repository and associated resources. *Nucleic Acids Res.* **37**, D387–D392.

Kim, H. and Ralph, J. (2010) Solution-state 2D NMR of ball-milled plant cell wall gels in DMSO–d_6/pyridine–d_5. *Org. Biomol. Chem.* **8**, 576–591.

Kim, H., Ralph, J. and Akiyama, T. (2008) Solution-state 2D NMR of ball--milled plant cell wall gels in DMSO–d_6. *Bioenergy Res.* **1**, 56–66.

Kondo, T., Mizuno, K. and Kato, T. (1990) Cell wall-bound *p*–coumaric and ferulic acids in Italian ryegrass. *Can. J. Plant Sci.* **70**, 495–499.

Kupce, E. and Freeman, R. (2007) Compensated adiabatic inversion pulses: broadband INEPT and HSQC. *J. Magn. Reson.* **187**, 258–265.

Lallemand, L.A., Zubieta, C., Lee, S.G., Wang, Y., Acajjaoui, S., Timmins, J., McSweeney, S., Jez, J.M., McCarthy, J.G. and McCarthy, A.A. (2012) A structural basis for the biosynthesis of the major chlorogenic acids found in coffee. *Plant Physiol.* **160**, 249–260.

Lin, S.Y. and Dence, C.W. (1992) *Methods in Lignin Chemistry*. Heidelberg, Germany: Springer-Verlag.

Lu, F. and Ralph, J. (1999) Detection and determination of *p*–coumaroylated units in lignins. *J. Agric. Food Chem.* **47**, 1988–1992.

Lu, F. and Ralph, J. (2003) Non-degradative dissolution and acetylation of ball-milled plant cell walls; high-resolution solution-state NMR. *Plant J.* **35**, 535–544.

Madden, T.L. (2002) The BLAST sequence analysis tool. In *The NCBI Handbook* (McEntyre, J. and Ostell, J., eds). Bethesda, MD: National Center for Biotechnology Information.

Marita, J.M., Vermerris, W., Ralph, J. and Hatfield, R.D. (2003) Variations in the cell wall composition of maize *brown midrib* mutants. *J. Agric. Food Chem.* **51**, 1313–1321.

Miki, D. and Shimamoto, K. (2004) Simple RNAi vectors for stable and transient suppression of gene function in rice. *Plant Cell Physiol.* **45**, 490–495.

Miki, D., Itoh, R. and Shimamoto, K. (2005) RNA silencing of single and multiple members in a gene family of rice. *Plant Physiol.* **138**, 1903–1913.

Morrison, T.A., Jung, H.G., Buxton, D.R. and Hatfield, R.D. (1998) Cell-wall composition of maize internodes of varying maturity. *Crop Sci.* **38**, 455–460.

Mueller-Harvey, I., Hartley, R.D., Harris, P.J. and Curzon, E.H. (1986) Linkage of *p*–coumaryl and feruloyl groups to cell wall polysaccharides of barley straw. *Carbohydr. Res.* **148**, 71–85.

Obst, J.R. (1982) Guaiacyl and syringyl lignin composition in hardwood cell components. *Holzforschung*, **36**, 143–152.

Petrik, D. L., Karlen, S. D., Cass, C. L. *et al.* (2014) p-Coumaroyl-CoA:monolignol transferase (PMT) acts specifically in the lignin biosynthetic pathway in Brachypodium distachyon. *Plant J.* **77**, 713–726.

Peitsch, M.C. (1995) Protein modeling by e–mail. *Nat. Biotechnol.* **13**, 658–660.

Penning, B.W., Hunter, C.T. III, Tayengwa, R. *et al.* (2009) Genetic resources for maize cell wall biology. *Plant Physiol.* **151**, 1703–1728.

Piston, F., Uauy, C., Fu, L., Langston, J., Labavitch, J. and Dubcovsky, J. (2010) Down-regulation of four putative arabinoxylan feruloyl transferase genes from family PF02458 reduces ester-linked ferulate content in rice cell walls. *Planta*, **231**, 677–691.

Ralph, J., Landucci, W.L., Ralph, S.A. and Landucci, L.L. (1993) NMR database of lignin and cell wall model compounds. URL http://ars.usda.gov/Services/docs.htm?docid=10491 (accessed on 15 April 2014).

Ralph, J., Hatfield, R.D., Quideau, S., Helm, R.F., Grabber, J.H. and Jung, H.J.G. (1994) Pathway of *p*–coumaric acid incorporation into maize lignin as revealed by NMR. *J. Am. Chem. Soc.* **116**, 9448–9456.

Ramakers, C., Ruijter, J.M., Deprez, R.H.L. and Moorman, A.F.M. (2003) Assumption-free analysis of quantitative real-time polymerase chain reaction (PCR) data. *Neurosci. Lett.* **339**, 62–66.

Sekhon, R.S., Lin, H., Childs, K.L., Hansey, C.N., Buell, C.R., de Leon, N. and Kaeppler, S.M. (2011) Genome-wide atlas of transcription during maize development. *Plant J.* **66**, 553–563.

Soderlund, C., Descour, A., Kudrna, D. *et al.* (2009) Sequencing, mapping, and analysis of 27,455 maize full-length cDNAs. *PLoS Genet.* **5**, e1000740.

Sullivan, M. (2009) A novel red clover hydroxycinnamoyl transferase has enzymatic activities consistent with a role in phaselic acid biosynthesis. *Plant Physiol.* **150**, 1866–1879.

Takahama, U. and Oniki, T. (1997) Enhancement of peroxidase-dependent oxidation of sinapyl alcohol by an apoplastic component, 4–coumaric acid ester isolated from epicotyls of *Vigna angularis* L. *Plant Cell Physiol.* **38**, 456–462.

Takahama, U., Oniki, T. and Shimokawa, H. (1996) A possible mechanism for the oxidation of sinapyl alcohol by peroxidase-dependent reactions in the apoplast: enhancement of the oxidation by hydroxycinnamic acids and components of the apoplast. *Plant Cell Physiol.* **37**, 499–504.

Walker, A.M., Hayes, R.P., Youn, B., Vermerris, W., Sattler, S.E. and Kang, C. (2013) Elucidation of the structure and reaction mechanism of sorghum hydroxycinnamoyltransferase and its structural relationship to other coenzyme A-dependent transferases and synthases. *Plant Physiol.* **162**, 640–651.

Wang, H., Nussbaum-Wagler, T., Li, B., Zhao, Q., Vigouroux, Y., Faller, M., Bomblies, K., Lukens, L. and Doebley, J.F. (2005) The origin of the naked grains of maize. *Nature*, **436**, 714–719.

Wang, L., Xie, W., Chen, Y. *et al.* (2010) A dynamic gene expression atlas covering the entire life cycle of rice. *Plant J.* **61**, 752–766.

Withers, S., Lu, F.C., Kim, H., Zhu, Y.M., Ralph, J. and Wilkerson, C.G. (2012) Identification of grass-specific enzyme that acylates monolignols with *p*–coumarate. *J. Biol. Chem.* **287**, 8347–8355.

Yang, U.M. and Fujita, H. (1997) Changes in grass lipid fractions and fatty acid composition attributed to hay making. *Grassland Sci.* **42**, 289–293.

Ye, J., Coulouris, G., Zaretskaya, I., Cutcutache, I., Rozen, S. and Madden, T.L. (2012) Primer-BLAST: a tool to design target-specific primers for polymerase chain reaction. *BMC Bioinformatics*, **13**, 134.

Yelle, D.J., Ralph, J. and Frihart, C.R. (2008) Characterization of nonderivatized plant cell walls using high-resolution solution-state NMR spectroscopy. *Magn. Reson. Chem.* **46**, 508–517.